

# Phase Space Tomography of Classical and Nonclassical Vibrational States of Atoms in an Optical Lattice

J.F. Kanem, S. Maneshi, S.H. Myrskog, and A.M. Steinberg

*Centre for Quantum Information & Quantum Control and Institute for Optical Sciences,*

*Department of Physics, University of Toronto, Canada*

(Dated: June 15, 2005)

## Abstract

Atoms trapped in optical lattice have long been a system of interest in the AMO community, and in recent years much study has been devoted to both short- and long-range coherence in this system, as well as to its possible applications to quantum information processing. Here we demonstrate for the first time complete determination of the quantum phase space distributions for an ensemble of  $^{85}\text{Rb}$  atoms in such a lattice, including a negative Wigner function for atoms in an inverted state.

arXiv:quant-ph/0506140v1 16 Jun 2005

## I. INTRODUCTION

Much of the excitement and promise of new fields such as quantum information processing would not be possible without the development of sophisticated techniques for manipulating and measuring quantum systems. In systems such as ion traps, quantum dots, Bose-Einstein condensates, and entangled photons, it is the fact that quantum states can be accurately prepared and observed which has enabled a wide range of experimental advances, and held out hope for the creation of practical quantum technologies. In such systems, quantum states inevitably evolve into partially mixed states, which can be characterized either by a density matrix, in the case of a finite-dimensional Hilbert space, or by phase space quasi-probability distributions such as the Wigner function[1] or the Husimi distribution[2]. Techniques for extracting these functions, generally referred to as “quantum tomography,” have long been a topic of active research, in the context of the electromagnetic field[3, 4], Rydberg states[5], neutral atoms[6, 7], dissociating molecules[8], entangled photons[9, 10, 11], and ion traps[12, 13].

One system which has led to many interesting effects and proposals is the “optical lattice,” in which atoms are trapped in a periodic potential formed by a standing wave of light beams[14, 15, 16]. This analog condensed-matter system has been used to study Bragg scattering[17], precision measurement using atom interferometry[18], the fragmentation of Bose condensates[19, 20], squeezed states of atomic motion[21], quantum feedback[22], the Mott insulator transition[23], and quantum logic gates[24, 25, 26], to name only a few examples. Typical probes of the system include the Bragg scattering of probe beams, which is sensitive to the localization  $\langle X^2 \rangle$  of the atoms; the time-varying transmission of the lattice beams themselves, which is sensitive to the instantaneous force exerted on the atoms, related to the centre-of-mass position  $\langle X \rangle$  in each well; and atom-interferometric probes of long-range coherence. Here we present for the first time a complete characterisation of the quantum state of atoms trapped in optical-lattice wells, by extracting the Husimi and Wigner distributions for atoms in several different initial states. In particular, we demonstrate the “nonclassical” Wigner function for atoms with a population inversion, whose negative value at the origin is analogous to that for the 1-photon Fock state and for the excited state of the single ion in a trap.

## II. THEORY

The Husimi distribution is a well known quasi-probability distribution related to a state's density matrix  $\rho$  by the equation  $Q(\alpha) = \frac{1}{\pi} \langle \alpha | \rho | \alpha \rangle$ , where  $|\alpha\rangle$  is a coherent state, that is, a Gaussian distribution centered at  $\alpha$ , with minimum-uncertainty width which can be defined by a specified harmonic oscillator. It has the practical advantage that its value for a particular  $\alpha$  is an observable and can be obtained directly with one measurement. Because it is always real and always positive it is sometimes referred to as a classical quasi-probability distribution.

The Wigner distribution, which has a one-to-one correspondence with the Husimi distribution, is particularly useful for identifying nonclassical states such as Fock or inverted states, for which it takes on negative value (as in fact it does for any non-Gaussian states). It can be defined by the expression  $W(x, p) = \frac{1}{\pi} \int_{-\infty}^{+\infty} \langle x + q | \rho | x - q \rangle \exp[-2ipq] dq$  [27]. The Wigner distribution is unique in that it allows one to determine the marginal probability distribution of either coordinate by integrating over the other:  $P(x) = \int W(x, p) dp$  and  $P(p) = \int W(x, p) dx$ .

The measurement of these quasi-probability distributions becomes particularly simple in a harmonic oscillator. The Husimi distribution can be measured by evaluating the expression

$$Q(|\alpha|, \theta) = \frac{1}{\pi} \langle \alpha | \rho | \alpha \rangle = \frac{1}{\pi} \langle 0 | D^\dagger(|\alpha|) R(\theta) \rho R^\dagger(\theta) D(|\alpha|) | 0 \rangle, \quad (1)$$

where  $\theta = \arg\{\alpha\}$ . That is, instead of projecting the unknown state  $\rho$  onto a coherent state  $\alpha$ , one can perform position displacement,  $D(|\alpha|)$ , and rotation,  $R(\theta)$ , operations on the unknown state and measure the overlap of the resulting state onto the ground state  $|0\rangle$ , which is a straightforward process in our experiment. Applying the displacement operator amounts to physically displacing the state a distance of  $x = 2x_0 |\alpha|$ , where  $x_0 = \left(\frac{\hbar}{2m\omega}\right)^{1/2}$  is the ground state width of a particle of mass  $m$  in a harmonic oscillator of frequency  $\omega$ . In a harmonic oscillator  $R(\theta) = \exp[-ia^\dagger a \theta]$  can be implemented by letting the state evolve under  $\mathcal{H} = \hbar\omega (a^\dagger a + \frac{1}{2})$  for a time  $t = \theta/\omega$ . How these operations are performed experimentally and how the ground state population of a state is measured will be described in section III.

The measurement of the Wigner distribution is simplified by recognizing that for any symmetric non-degenerate potential and, in particular, in a harmonic oscillator,  $W(0, 0) =$

$\frac{1}{\pi} \int_{-\infty}^{+\infty} \langle q | \rho | -q \rangle dq = \frac{1}{\pi} \sum_{n=0}^{\infty} (-1)^n \langle n | \rho | n \rangle$ . For values away from the origin the displacement and rotation operators can once again be utilized:

$$W(x, p) = W(2x_0 \Re(\alpha), 2p_0 \Im(\alpha)) = \frac{1}{\pi} \sum_{n=0}^{\infty} (-1)^n p(n|\alpha), \quad (2)$$

where  $p_0 = \sqrt{m\hbar\omega/2}$  and  $p(n|\alpha) = \langle n | D^\dagger(|\alpha\rangle) R(\theta) \rho R^\dagger(\theta) D(|\alpha\rangle | n \rangle$  is the probability of finding the particle to be in state  $n$  after the application of the rotation and displacement operators to the unknown state  $\rho$ . Therefore, the determination of the Wigner distribution is reduced to performing population measurements after applying displacement and rotation operators. This is similar to the reconstruction of the Husimi distribution except that the final population measurement requires the measurement of all states, ( $|0\rangle, |1\rangle, |2\rangle, \dots$ ), not just the population of the ground state.

### III. IMPLEMENTATION

#### A. Optical Lattice Specifications

A 1-D optical lattice is formed by the counter-propagating components of two laser beams resulting in an intensity interference pattern of the form  $I(x) = I_0 \cos^2(kx \sin(\frac{\gamma}{2}))$ , where  $k = \frac{2\pi}{\lambda}$  is the wave vector of the laser and  $\gamma$  is the angle of intersection of the two beams. This standing light wave induces a light shift on the atoms resulting in a potential  $U(x) = I(x) \frac{\hbar\Gamma^2}{4\Delta I_s}$  where  $\Delta$  is the detuning of the laser light from atomic resonance and  $\Gamma$  and  $I_s$  are the natural line-width and saturation intensity of the atom respectively. Of importance to this experiment is the fact that the individual wells of an optical lattice can be approximated as harmonic oscillators. Therefore the theory of Husimi and Wigner distribution measurements in harmonic oscillators can be applied here. The oscillation frequency in each well  $\omega$ , and lattice depth  $U_0$ , are related by the equation  $\omega = \frac{4k_L}{\pi} \sqrt{\frac{U_0}{m}}$ . We find directly by measuring the period of Ramsey fringes created by inducing oscillations with a spatial shift of the sinusoidal potential[28].

Our experiment starts with a cloud of  $^{85}\text{Rb}$  atoms in a magneto optical trap (MOT) which are then cooled in an optical molasses to a temperature on the order of  $10\mu\text{K}$ . The optical lattice is turned on during the MOT stage as cooling in the presence of the lattice increases the lattice loading efficiency. The two laser beams intersect at an angle of  $\gamma = 49.6^\circ$ ,

resulting in a lattice vector of  $k_L = \frac{2\pi}{\lambda} \sin\left(\frac{\gamma}{2}\right) = \frac{\pi}{a} = 3.38 \cdot 10^6 m^{-1}$ , where  $\lambda = 780nm$  is the wavelength of the lattice light and  $a = 0.93\mu m$  is the spatial period of the lattice. The lattice has a detuning of  $\Delta \simeq 2\pi \cdot 25GHz$  from the  $F = 3 \Rightarrow F' = 4$   $D2$  trapping line of  $^{85}Rb$  so as to make the scattering rate negligible and to allow the sinusoidal lattice potential to be treated as conservative. The lattice is tailored to support 2 – 4 bound states, depending on the experiment, which means a depth of  $U_0 \simeq 10 - 40E_r$  where  $E_r = \frac{\hbar^2 k_L^2}{2m}$  is the scaled recoil energy in the lattice direction. The lattice is formed in the vertical direction so that atoms in unbound states will, in a time of  $\lesssim 10ms$ , leave the interaction region due to the pull of gravity. Each of the lattice beams passes through an acousto-optic modulator (AOM). By controlling the frequency and phase of the signal with which we drive each AOM independently we are able to control the position, velocity and acceleration of the lattice. Shifting the relative phase of the lattice beams by  $\phi$  displaces the lattice (or, in the rest frame of the lattice, displaces the atoms) by a distance  $d = a\phi/2\pi$ . Spatial shifts, used for the displacement operators  $D(|\alpha\rangle)$ , can be applied with a resolution on the order of  $1nm$ . Displacements as large as twice the lattice spatial period occur in a time of  $\lesssim 0.5\mu s$ . With typical oscillation frequencies of  $\omega/2\pi \simeq 10^4 Hz$ , this time interval for a shift can be considered to be instantaneous.

## B. State Preparation

The preparation of the states whose quasi-probability distributions we shall measure requires two steps. The first is to filter out the ground state. By lowering the intensity of the lattice beams over a time of  $10ms$  until only one bound state is supported, and keeping it there for  $5ms$ , all atoms in higher states become unbound and fall out of the interaction region due to gravity. Afterwards we raise the intensity back to its original level but are left with the ground state in each well, with a typical contamination of the first excited state of about 5 – 15%. A more detailed explanation of our ground state preparation and measurement process can be found in reference [28] and a similar technique is described in reference [29]. The implementation of the second part of the state preparation depends on what state we wish to prepare.

In this paper we prepare and measure three states: a ground state, a near coherent state and a state with a population inversion. For the ground state no further action is necessary

as it was prepared in the filtering stage. A near coherent state,  $|\beta\rangle$ , is prepared by shifting the potential by  $\delta x = \frac{a}{6} = 0.155\mu m$  (or a  $60^\circ$  phase shift). The magnitude of  $\beta$  is related to the displacement by  $|\beta| = \delta x \left(\frac{m\omega}{2\hbar}\right)^{1/2} = 0.88$ . For both the ground and coherent state a lattice depth of  $37E_r$  was chosen, supporting 4 bound states with an oscillation frequency of  $\omega = 48.33kHz$ . The deviation of the near coherent state which we prepare from an actual coherent state is due to the finite depth of the lattice. With only 4 bound states only the first 4 terms of the coherent state are present in the lattice. This does not significantly detract from the validity of the approximation, as the amplitude of the  $n^{\text{th}}$  term in a harmonic oscillator coherent state is  $\exp[-|\beta|^2/2] \frac{1}{\sqrt{n!}} |\beta|^n$ , which when  $|\beta| = 0.88$  is quite small for  $n \geq 4$ . This state was allowed to rotate in the potential for a time  $t = 20\mu s$ , giving it a rotation of  $\theta = 0.97$  radians.

Creation of an inverted state begins with the preparation of the ground state, this time in a lattice containing only two bound states ( $\omega = 32.2kHz$ ). Next, the potential is given a  $60^\circ$  phase shift ( $0.155\mu m$ ), held there for  $80\mu s$  and then shifted back to its original position. We have found that this process excites a large number of atoms into higher states[30]. After waiting several milliseconds in order to let unbound atoms leave the interaction region we are left with what will be shown to be an incoherent mixture of ground and first-excited-state atoms in a ratio of roughly 3 to 7.

### C. State Measurement

Here we describe the process used to determine the Husimi distribution for the ground state and coherent state. As per equation 1 the measurement of  $Q(|\alpha|, \theta)$  takes three steps. First, we allow the atoms to undergo free evolution for a time  $t$  to let the state oscillate in the harmonic-like potential for a rotation of  $\theta = \omega t$  in phase space. We use a total of 27 angles (or wait times,  $t$ ) separated by 0.24 radians (or  $5\mu s$ ), spanning a range of  $\theta \in [0, 2\pi]$  ( $\delta t \in [0, 130]\mu s$ ). Second, a displacement of  $x = 2x_0|\alpha|$  is applied to the lattice. This is the displacement operator,  $D(|\alpha|)$ . A total of 19 different displacements are used, each separated by  $25.8nm$  or a  $10^\circ$  phase shift of the potential for a total range of  $x \in [0, 465]nm$  or  $[0, 180]$  degrees. Along with the phase component, the total number of measurements is then 513 not including repeated measurements for statistical analysis and averaging. Next, a projection of this new state onto the ground state is performed. This first requires the

same process that was used to filter the ground state during the state preparation: the lattice laser intensity is lowered until only the ground state remains. After waiting  $\sim 20ms$  in order to let the unbound atoms become spatially separated from those still bound the atoms are illuminated with resonant light, and their fluorescence collected in a CCD camera. With this image the relative population of ground state atoms, as a fraction of total atom number, is measured.

Figure 1 is a phase space diagram of the Husimi distribution for the coherent state. As expected, it is a Gaussian displaced from the origin by  $|\beta| = 0.88$  at an angle of roughly  $55^\circ$ . Since a coherent state is merely a ground state displaced from the origin in phase space both distributions should have the same width. Figure 2 shows a cross section of the Husimi distribution for the ground state along with one of the coherent state. Fits of these Gaussians give *rms* widths of  $144nm$  and  $147nm$  and peaks of  $0.267$  and  $0.257$  for the ground and coherent states respectively. Husimi distributions, by definition, are normalized. By integrating the curve shown in figure 1 we find from  $\int Q(|\alpha|, \theta) |\alpha| d|\alpha| d\theta = \int Q\left(\frac{r}{2x_{rms}}, \theta\right) \frac{r}{4x_{rms}^2} dr d\theta = 1$  that  $x_{rms} = 96.3nm$ . Here we find a surprising result. The ground state width of a harmonic oscillator of this frequency is  $x_0 = \left(\frac{\hbar}{2m\omega}\right)^{1/2} = 88.0nm$  but we find  $x_{rms} = 96.3nm = 1.09 \cdot x_0$ . We believe that this discrepancy is due to inhomogeneities in the intensity of our lattice beams. We have separately measured the dephasing time  $T_2$  to be on the order of 2 or 3 oscillation periods in our lattice[28, 30], implying  $\Delta\omega \approx 0.4\omega$ . As  $x_0^2 = \hbar/2m\omega$ , we expect the rms width of our atom clouds to be  $x_{rms} = (\hbar/2m)\langle 1/\omega \rangle = x_0^2[1 + (\Delta\omega/\omega)^2 + (\Delta\omega/\omega)^4 + \dots]$ . For  $\Delta\omega/\omega \sim 0.4$ , this means  $x_{rms} \approx 1.08x_0$ , consistent with our observations.

In addition, the peak of the Husimi distribution of a true ground state is  $\frac{1}{\pi}$ . Our measured distribution has a peak value of  $0.267 = 0.84/\pi$ , obtained from a direct measurement of the ground-state population to be 84%. A harmonic-oscillator state with 16% population in the first excited state, when the ground-state width is taken to be  $x_{rms}$  as calculated above, has a Husimi distribution with a width of 141 nm, consistent with our measured value.

Following equation 2 the Wigner distribution for the inverted state is measured by first applying the rotation and displacement operators  $R(\theta)$  and  $D(|\alpha|)$ , as in the Husimi reconstruction. For the rotation operators we sample 41 different rotation angles separated by 0.16 radians spanning a range of  $\theta \in [0, 2\pi]$  equivalent to waiting times in the range  $\delta t \in [0, 200] \mu s$  with a resolution of  $5 \mu s$ . We again use 19 different spatial shifts for the displacement op-

erators with a range of  $x \in [0, 465] \text{ nm}$  giving a total number of 779 measurements for the Wigner measurement.

After the rotation and displacement operations are implemented, the state populations must be measured. Since the lattice holds two bound states any atoms excited to higher states by the rotation and displacement operators become unbound. After waiting  $5 \text{ ms}$  in order to let these atoms become spatially separated we once again lower the lattice laser intensity until only one bound state remains. After waiting another  $20 \text{ ms}$  in order to let these first-excited-state atoms leave the interaction region we then capture a fluorescence image. From this image we determine the ground and first-excited-state populations as well as how many atoms were in states  $n \geq 2$ . Therefore we are able to construct the Wigner distribution with the following caveat: measurements of  $W(x, p)$  become increasingly uncertain for values for which the displacement operator  $D(|\alpha|)$  excites more atoms into  $n \geq 2$ , since only the first two terms of equation 2 are known exactly.

Figure 3 shows a cross section of our best estimate of the Wigner distribution:  $W'(x, 0) \equiv \frac{1}{\pi} (p(0|\alpha) - p(1|\alpha))$ . At the origin we see that the distribution is negative, a nonclassical signature which is characteristic of a population inversion. The inset shows the absolute upper and lower bounds, based on our data, of the Wigner distribution due to our lack of knowledge about the populations of states higher than  $n = 1$ . The upper bound is obtained by assuming that all atoms lost during the displacement and rotation operators were in the 2nd excited state;  $\frac{1}{\pi} (p(0|\alpha) - p(1|\alpha) + p(n > 1|\alpha))$ , while the lower is constructed by assuming they were in the 3rd;  $\frac{1}{\pi} (p(0|\alpha) - p(1|\alpha) - p(n > 1|\alpha))$ . Of course neither one of these extremes can be the case as they are not physical. It is known that the Wigner distribution for any state must go to zero as  $x, p \rightarrow \infty$ . In addition, one can get a sense of the magnitude of the disagreement between  $W$  and  $W'$  by investigating the normalisation of the three curves;  $\int W'(x, p) dx dp = 0.42$ , which is clearly not consistent with 1. The same normalisation integral, however, gives values of 10.32 and  $-9.49$  for the upper- and lower-bound curves, respectively. Clearly, the real Wigner function lies between  $W'$  and the upper bound, but much closer to the former. Theoretically, one expects a significant additional contribution from the second excited state for  $|\alpha| \sim 1$ , but for larger values of  $|\alpha|$  this should be cancelled out by higher populations in the third excited state. Near the origin, there was no population in states with  $n \geq 2$ , so there is no uncertainty.

Figure 4 shows a 3-D representation of the Wigner distribution measurement. Note the



rotational symmetry, which indicates a lack of coherence between energy eigenstates. Usually processes such as the displacement operator create coherent superpositions of states such as in the case with our presented Husimi distribution. The lack of any coherence properties here is due to the combination of dephasing processes inherent in our optical lattice[28] and the long delay between the population inversion creation and the time of measurement. Therefore the result of our state creation, as shown by figures 3 and 4 is an incoherent mixture of ground and 1st excited state atoms with most atoms being in the latter, as evidenced by the negative component of the Wigner distribution.

#### IV. CONCLUSION

Making use of a newly developed technique to measure state populations of the vibrational states of atoms in  $1\text{-}\mu\text{m}$  lattice wells, and our ability to perform arbitrary translations in phase space, we have reconstructed Husimi and Wigner phase space distributions for atoms in ground, coherent, and inverted states of oscillation in an optical lattice. This is the first complete quantum characterisation of the state of motion of atoms in such a system. The ground and coherent states are largely consistent with expectations, possessing essentially the same shape and width, although they indicate both some admixture of the excited state, which is understandable in light of our preparation procedure, and an apparent underestimate of the width of the ground-state wave function relative to the experimental measurement, which is probably due to inhomogeneities in the lattice beams. We observe a nonclassical signature in the Wigner function, reaching a maximum negative value of  $-0.12$  at the origin, in the case of the inverted distribution.

#### V. ACKNOWLEDGMENTS

We would like to thank Matt Partlow for helpful discussions and assistance with the manuscript, and John Sipe for many informative conversations about Wigner distributions. We acknowledge financial support from NSERC, from the CIAR, and from the DARPA QuIST program (managed by the AFOSR under agreement no. F49620-01-1-0468).

- 
- [1] E.P. Wigner, Phys. Rev. **40**, 749 (1932).
- [2] K. Husimi, Proc. Phys. Soc. Japan **22**, 264 (1940).
- [3] D.T. Smithey, M. Beck, A. Faridani, M.G. Raymer, Phys. Rev. Lett. **70**, 1244 (1993).
- [4] A.I. Lvovsky, H. Hansen, T. Aichele, O. Benson, J. Mlynek, S. Schiller, Phys. Rev. Lett. **87**, 050402 (2001).
- [5] T.J. Dunn, I.A. Walmsley, S. Mukamel, Phys. Rev. Lett. **74**, 884 (1995)
- [6] G. Klose, G. Smith, P.S. Jessen, Phys. Rev. Lett. **86**, 4721 (2001).
- [7] C. Kurtsiefer, T. Pfau, J. Mlynek, Nature **386**, 150 (1997).
- [8] E. Skovsen, H. Stapelfeldt, S. Juhl, K. Mølmer, Phys. Rev. Lett. **91**, 090406 (2003)
- [9] D.F.V. James, P.G. Kwiat, W.J. Munro, A.G. White, Phys. Rev. A **64**, 052312 (2001).
- [10] J.B. Altepeter, D. Branning, E. Jeffrey, T.C. Wei, P.G. Kwiat, R.T. Thew, J.L O'Brien, M.A. Nielson, A.G. White, Phys. Rev. Lett. **90**, 193601 (2003).
- [11] M.W. Mitchell, C.W. Ellenor, S. Schneider, A.M. Steinberg, Phys. Rev. Lett. **91**, 120402 (2003).
- [12] J.F. Poyatos, R. Walser, J.I. Cirac, P. Zoller, R. Blatt, Phys. Rev. A **53**, 1966 (1996).
- [13] D. Leibfried, D.M. Meekhof, B.E. King, C. Monroe, W.M. Itano, D.J. Wineland, Phys. Rev. Lett. **77**, 4281 (1996).
- [14] N.P. Bigelow, M.G. Prentiss, Phys. Rev. Lett. **65**, 29 (1990).
- [15] C.I. Westbrook, R.N. Watts, C.E. Tanner, S.L. Rolston, W.D. Phillips, P.D. Lett, Phys. Rev. Lett. **65**, 33 (1990).
- [16] P.S. Jessen, I. H. Deutsch, Adv. Atm. Mol. Opt. Phys. **37**, 95 (1996).
- [17] G. Birkel, M. Gatzke, I.H. Deutsch, S.L. Rolston, W.D. Phillips, Phys. Rev. Lett. **75**, 2823 (1995).
- [18] M.J. Snadden, J.M. McGuirk, P. Bouyer, K.G. Haritos, M.A. Kasevich, Phys. Rev. Lett. **81**, 971 (1998).
- [19] R.W. Spekkens, J.E. Sipe, Phys. Rev. A **59**, 3868 (1999).
- [20] C. Orzel, A.K. Tuchman, M.L. Fenselau, M. Yasuda, and M.A. Kasevich, Science **291**, 2386 (2001).
- [21] G. Raithel, G. Birkel, W.D. Phillips, and S.L. Rolston, Phys. Rev. Lett. **78**, 2928 (1997).

- [22] N.V. Morrow, S.K. Dutta, G. Raithel, Phys. Rev. Lett. **88**, 093003 (2002).
- [23] M. Greiner, O. Mandel, T. Esslinger, T.W. Hänsch, I. Bloch, Nature **415**, 39 (2002).
- [24] G.K. Brennen, I.H. Deutsch, P.S. Jessen, Phys. Rev. A **61**, 062309 (2000).
- [25] H.J. Briegel, T. Calarco, D. Jaksch, J.I. Cirac, P. Zoller, Journal Mod. Opt. **47**, 415 (2000).
- [26] O. Mandel, M. Greiner, A. Widera, T. Rom, T. Hänsch, I. Bloch, Phys. Rev. Lett. **91**, 010407 (2003).
- [27] U. Leonhardt, Phys. Rev. A **53**, 2998 (1996).
- [28] S.H. Myrskog, J.K. Fox, M.W. Mitchell, A.M. Steinberg, "Quantum Process Tomography on Vibrational States of Atoms in an Optical Lattice" accepted for publication in Phys. Rev. A.
- [29] T. Muller-Seydlitz, M. Hartl, B. Brezger, H. Hansel, C. Keller, A. Schnetz, R.J.C. Spreeuw, T. Pfau, J. Mlynek, Phys. Rev. Lett. **78**, 1038 (1997).
- [30] S. Maneshi, J.F. Kanem, M.J. Partlow, and A.M. Steinberg, in preparation.

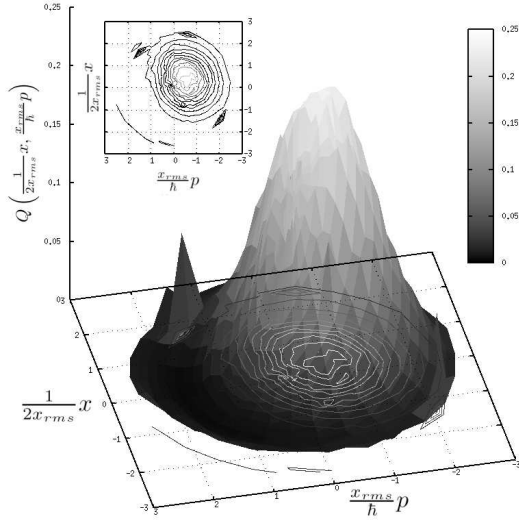


Figure 1: Phase space representation of the Husimi distribution of a coherent state  $||\beta\rangle, \theta\rangle$  for  $|\beta| = 0.88$ ,  $\theta = 0.97$ . From the contour plot in the inset one can see the displacement of the Gaussian from the origin. Axis units are in  $x/2x_{rms}$  where  $x_{rms} = 96.3nm$ .

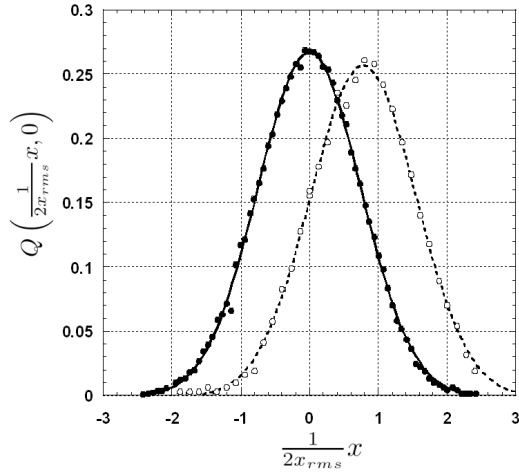


Figure 2: Cross sections of the Husimi distributions of the ground state (closed circles) and coherent state (open circles). As expected they have virtually the same width but the coherent state is displaced from the origin. In addition, the height and width, when compared to the true ground state of a harmonic oscillator of this frequency, show that there is some contamination of the state by first excited state atoms.

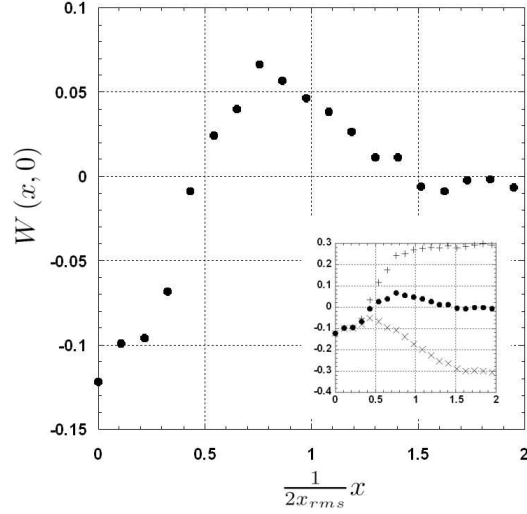


Figure 3: Cross section of the measured Wigner distribution. Negative values at the origin are indicative of a population inversion. Inset shows absolute upper (+) and lower ( $\times$ ) bounds of the distribution as explained in the text. Axis units are in  $x/2x_{rms}$  where  $x_{rms} = 119.4nm$

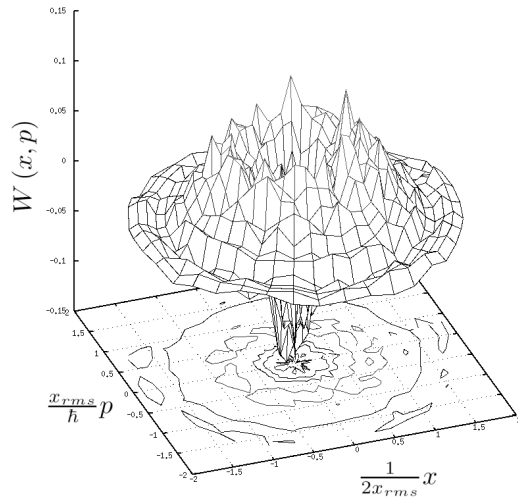


Figure 4: 3-D image of the measured Wigner distribution. Of note is the cylindrical symmetry showing a lack of coherence between the component energy eigenstates.